



Cite this: *Dalton Trans.*, 2026, **55**, 2400

Recent progress in Pt(II)- and Ir(III)-complex-based chemical sensors for detecting picric acid

Xiaoran Yang,^a Qinglong Zhang,^a Boyuan Miao*^b and Chun Liu *^a

The efficient detection of picric acid (PA) is of great significance in the fields of environmental protection and counter-terrorism. To date, a variety of metal complexes have been developed for sensing PA. Among them, Pt(II) and Ir(III) complexes have attracted much attention due to their excellent photostability and tunable luminescence properties. This review provides a systematic overview of the recent progress in the molecular structure design of Pt(II) and Ir(III) complexes and their effects on the performance of PA detection in different solvent systems, especially in aqueous media. In addition, the directions and prospects for the detection of PA are presented and discussed. This review affords important theoretical references and application insights for the field of explosives detection and environmental pollution monitoring.

Received 3rd September 2025,
Accepted 19th December 2025

DOI: 10.1039/d5dt02114f

rsc.li/dalton

Introduction

Picric acid (PA) is an important raw material for producing various chemicals. Its unique chemical and physical properties make it useful in military, pharmaceutical, dye and other industries.^{1,2} However, the high explosive, water-soluble and bio-toxic properties of PA make it a serious threat to public safety and the ecological environment. Its residues can contaminate water and soil through wastewater discharge and can accumulate in living organisms, causing skin allergies, liver and kidney damage, and other diseases.^{3–5} Therefore, the development of highly sensitive and selective methods for the detection of PA is of great significance for human health and environmental protection.

Over the past decades, various methods have been developed for the detection of PA, such as electrochemical methods,⁶ Raman spectroscopy,⁷ mass spectrometry⁸ and photoluminescence.⁹ Among these, the photoluminescence method has become one of the most important means for the efficient detection of PA due to its advantages of fast response time, high sensitivity, real-time monitoring and easy operation.¹⁰ In the photoluminescence method, metal complex sensors exhibit outstanding tunable photophysical properties. Through precise molecular design (*e.g.*, modifying the metal center or ligand structure), their emission wavelengths, quantum yields, and excited-state lifetimes can be systematically controlled to enhance detection performance. These strategies are typically more explicit and direct than those for organic conjugated systems. Additionally, they exhibit out-

standing chemical stability and photostability, which are crucial for long-term or repeated detection in practical applications.^{11–13} In view of these advantages, metal complexes such as Ru(II), Pt(II) and Ir(III) have been successfully used in the luminescence sensing of PA. In 2022, Khatua *et al.*¹⁴ reported a bis-heteroleptic Ru(II) complex **Ru1** using 4,7-bis(phenylthio)-1,10-phenanthroline and 1,10-phenanthroline as ligands (Fig. 1). The photophysical properties of **Ru1** were investigated by UV-vis absorption and emission spectroscopy. Photoluminescence (PL) spectroscopic studies showed that the luminescence quenching of **Ru1** in the presence of PA was highly selective. The limit of detection (LOD) for PA was calculated to be 4700 nM. To our knowledge, this is the first reported example of a Ru(II) complex for the selective detection

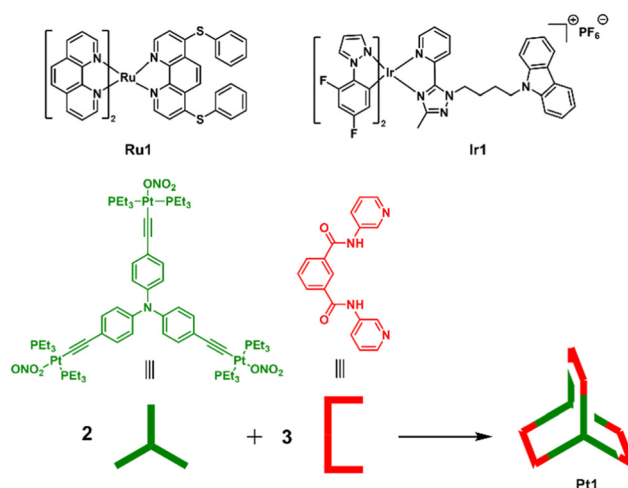


Fig. 1 Structures of **Ru1**, **Pt1**, and **Ir1**.

^aState Key Laboratory of Fine Chemicals, Dalian University of Technology, Linggong Road 2, Dalian 116024, China. E-mail: cliu@dlut.edu.cn

^bPetrochina Dalian Petrochemical Company, Shanzhong Street 1, Dalian 116031, China. E-mail: miaoboyuan35@163.com

of PA. In 2008, Mukherjee *et al.*¹⁵ prepared the complex **Pt1** (Fig. 1) with a triangular prism shape by self-assembly of a pre-designed organometallic platinum receptor with an organic clip-type ligand. **Pt1** represented the first instance of a prismatic derivative of a metallic triplanar receptor and was applied in explosives detection. The conjugated acetylenic and aromatic groups in the complex gave it strong luminescent properties, and efficient luminescence quenching was achieved through π -stacking and electron transfer interactions with PA, with the quenching constant (K_{SV}) of $4.8 \times 10^4 \text{ M}^{-1}$ in $\text{CH}_2\text{Cl}_2/\text{DMF}$. In 2013, Shan *et al.*¹⁶ reported a cationic Ir(III) complex **Ir1** (Fig. 1), which showed significant aggregation-induced phosphorescence emission (AIPE) activity¹⁷ in $\text{H}_2\text{O}/(\text{CH}_3)_2\text{CO}$. The emissive nanoaggregates of **Ir1** could be efficiently quenched by PA with a K_{SV} value of $7.2 \times 10^4 \text{ M}^{-1}$, making it a highly sensitive chemical sensor for explosives, which is the first reported AIPE-active Ir(III) complex for high-sensitivity detection of PA.

In this review, we focus on the recent advances in the detection of PA in different solvent systems based on various structural designs of Pt(II) and Ir(III) complexes in the past five years. To better understand the differences in the performances of metal complexes with different structures for the detection of PA, two summarized tables are provided (Tables 1 and 2). We hope to provide a general overview of the development of designing novel metal complexes and their detection performances for PA. Moreover, an overview of the abbreviations used in this review is given in Table 3.

Sensing mechanisms for PA detection by metal-complex sensors

Two common quenching mechanisms in luminescence quenching processes are static quenching and dynamic

Table 1 Luminescence quenching performance of Pt(II) complexes for PA detection

Pt(II) complexes	Systems	K_{SV} (M^{-1})	LOD (nM)	Detection mechanism	Ref.
Pt1	$\text{CH}_2\text{Cl}_2/\text{DMF}$	4.8×10^4	Unavailable	Unavailable	15
Pt2	CH_2Cl_2	1.3×10^5	301	Unavailable	26
Pt3	CH_3CN	5.2×10^4	2.8×10^3	Unavailable	27
Pt4	CH_3CN	4.1×10^4	3.3×10^3	Unavailable	27
Pt5	CH_3CN	1.1×10^5	2.5×10^3	Unavailable	27
Pt6	CH_3CN	5.5×10^4	2.4×10^3	Unavailable	27
Pt7	CH_3CN	3.8×10^4	3.0×10^3	Unavailable	27
Pt8	CH_3CN	6.8×10^4	2.3×10^3	Unavailable	27
Pt9	$\text{H}_2\text{O}/\text{CH}_3\text{CN}$	2.7×10^4	1.7×10^2	PET	32
Pt10	$\text{H}_2\text{O}/\text{CH}_3\text{CN}$	1.9×10^4	2.0×10^2	PET	32
Pt11	$\text{H}_2\text{O}/\text{CH}_3\text{CN}$	4.3×10^4	90	PET	32
Pt13	$\text{H}_2\text{O}/\text{CH}_3\text{CN}$	2.3×10^4	2.6×10^2	PET	33
Pt14	$\text{H}_2\text{O}/\text{THF}$	1.1×10^4	1.7×10^2	PET	36
Pt15	$\text{H}_2\text{O}/\text{THF}$	1.9×10^4	30	PET	36
Pt16	$\text{H}_2\text{O}/\text{THF}$	1.5×10^4	1.5×10^2	PET	36
Pt17	$\text{H}_2\text{O}/\text{THF}$	2.3×10^4	70	PET	38
Pt18	$\text{H}_2\text{O}/\text{THF}$	2.8×10^4	1.0×10^2	PET	38
Pt19	$\text{H}_2\text{O}/\text{THF}$	3.0×10^4	90	PET	38

Table 2 Luminescence quenching performance of Ir(III) complexes for PA detection

Ir(III) complexes	Systems	K_{SV} (M^{-1})	LOD (nM)	Detection mechanism	Ref.
Ir1	$\text{H}_2\text{O}/(\text{CH}_3)_2\text{CO}$	7.2×10^4	Unavailable	Unavailable	16
Ir2	CH_2Cl_2	2.4×10^3	2.9×10^4	PET	44
Ir3	CH_2Cl_2	1.9×10^4	1.0×10^4	Unavailable	45
Ir5	$\text{H}_2\text{O}/\text{THF}$	3.7×10^4	1.5×10^2	PET	46
Ir6	$\text{H}_2\text{O}/(\text{CH}_3)_2\text{CO}$	3.4×10^4	317	PET	48
Ir8	$\text{H}_2\text{O}/\text{CH}_3\text{CN}$	7.4×10^4	50.2	PET	50
Ir9	$\text{H}_2\text{O}/\text{CH}_3\text{CN}$	2.6×10^6	2.2	PET	50
Ir10	$\text{H}_2\text{O}/\text{CH}_3\text{CN}$	4.6×10^5	4.6	PET	52
Ir11	$\text{H}_2\text{O}/\text{CH}_3\text{CN}$	1.9×10^6	2.5	PET	52
Ir12	$\text{H}_2\text{O}/\text{CH}_3\text{CN}$	2.9×10^4	164	PET	54
Ir13	$\text{H}_2\text{O}/\text{CH}_3\text{CN}$	2.3×10^4	176	PET	54
Ir14	$\text{H}_2\text{O}/\text{CH}_3\text{CN}$	1.9×10^4	331	PET	54
Ir15	$\text{H}_2\text{O}/\text{THF}$	3.1×10^4	59	PET/FRET	56
Ir16	$\text{H}_2\text{O}/\text{THF}$	3.0×10^4	84	PET/FRET	56
Ir17	$\text{H}_2\text{O}/\text{THF}$	2.0×10^4	95	PET/FRET	56
Ir18	$\text{H}_2\text{O}/\text{CH}_3\text{CN}$	8.4×10^5	0.6	PET	57
Ir19	$\text{H}_2\text{O}/\text{CH}_3\text{CN}$	5.7×10^6	0.3	PET	57
Ir20	$\text{H}_2\text{O}/\text{CH}_3\text{CN}$	4.5×10^5	3.8	PET	57

Table 3 Summary of nomenclature

Abbreviation	Full name
AIE	Aggregation induced emission
AIPE	Aggregation induced phosphorescent emission
DFT	Density functional theory
DNP	2,4-Dinitrophenol
DNT	2,4-Dinitrotoluene
DPA	Diphenylamino
DPP	Diphenylphosphoryl
FRET	Förster resonance energy transfer
LOD	Limit of detection
LUMO	Lowest unoccupied molecular orbital
NMR	Nuclear magnetic resonance
PA	Picric acid, 2,4,6-trinitrophenol
PET	Photo-induced electron transfer
PL	Photoluminescence
TPA	Triphenylamino
HOMO	Highest occupied molecular orbital

quenching.¹⁸ Static quenching occurs when the luminescent molecules interact with the quencher to form a non-luminescent ground-state complex, thereby reducing the luminescence intensity of the molecules. In contrast, dynamic quenching refers to the excited state of the luminescent molecules returning to the ground state after colliding with the quencher, which may involve photo-induced electron transfer (PET)^{19–21} and Förster resonance energy transfer (FRET).^{22,23}

Photo-induced electron transfer (PET)

The strong electron-withdrawing nitro group of PA makes it an electron acceptor (A), while the metal complex acts as an electron donor (D). When the complex is excited by ultraviolet light, the electrons in its ground state jump from the highest occupied molecular orbital (HOMO) to the lowest unoccupied molecular orbital (LUMO), forming an excited state. During this process, if picric acid is present in the system and its

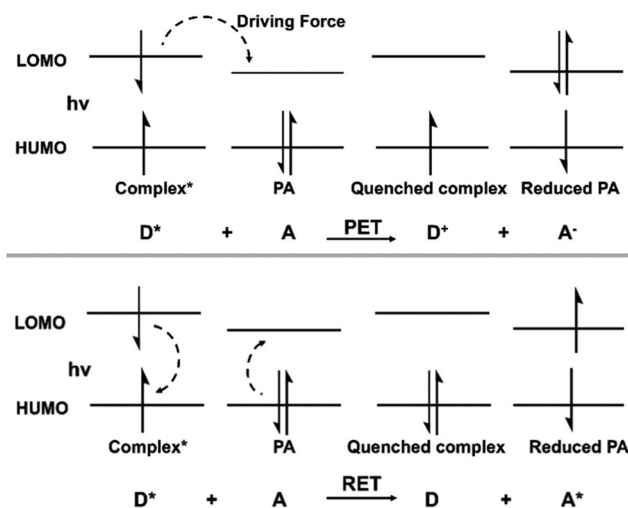


Fig. 2 Mechanisms of photo-induced electron transfer and resonance energy transfer.

LUMO energy level is significantly lower than the LUMO energy level of the excited state of the complex, the excited-state electrons are transferred from the LUMO of the complex to the LUMO orbital of the PA. This process prevents the excited-state electrons from returning to the ground state by radiative leaps, resulting in luminescence quenching. The driving force of this process originates from the LUMO energy level difference between the complex and the PA, and the PET mechanism has been widely demonstrated to be the core mechanism for PA detection (Fig. 2).

Förster resonance energy transfer (FRET)

In recent years, explosives detection technology based on the FRET mechanism has been developed rapidly, which significantly improves the sensitivity and selectivity of luminescent sensors through precise energy transfer modulation. As shown in Fig. 2, when the complex is excited, its excited-state energy is not released by radioluminescence, but the energy is transferred to the PA. According to the FRET mechanism, three conditions need to be satisfied for the efficiency of energy transfer: (1) the dipole orientation of the donor (complex) and the acceptor (PA) is matched; (2) the donor emission spectrum overlaps with the acceptor absorption spectrum; and (3) the donor–acceptor distance (R_0) is estimated to be in the range of 1–10 nm. The FRET efficiency (E) can be calculated by the equation $E = 1 - F/F_0 = R_0^6/(R_0^6 + r^6)$, where F and F_0 are the luminescence intensities with and without PA, respectively, and R_0 is the critical distance.

Recent advances in the detection of PA by Pt(II) complexes

Pt(II) complexes are characterized by a four-coordinated planar configuration, high quantum yields, long excited-state life-

times and large Stokes shifts, and their luminescence performances can be easily improved by adjusting the ligand structures; thus, they have become a hot spot of current research.^{24,25}

In 2020, Hou *et al.*²⁶ successfully constructed a platinum metallocycle-centered supramolecular network complex **Pt2**, by linking triphenylamino (TPA)-based metallocycles through dynamic covalent imine bonds. **Pt2** exhibited luminescence quenching after the addition of PA, and the luminescence of the complex was completely quenched when the concentration of PA was 4 times the equivalent of the complex's concentration. For the detection of PA in CH_2Cl_2 , K_{SV} value of **Pt2** was $1.3 \times 10^5 \text{ M}^{-1}$ and the LOD was 301 nM. In addition, this process could be easily observed with the naked eye. Thin films made of **Pt2** showed dramatic luminescence quenching after the addition of a drop of PA in CH_2Cl_2 . These results indicated that **Pt2** could be used as a chemical sensor for PA (Fig. 3).

In 2023, Hou *et al.*²⁷ constructed another series of bowtie-like cyclometalating complexes **Pt3–Pt8** with six triangular cavities (Fig. 3). Except for **Pt4**, all the complexes exhibited high absolute quantum yields in CH_3CN , which exceeded 98%. In addition, **Pt3–Pt8** all showed sensitive luminescence responses to PA with K_{SV} values of 5.2×10^4 , 4.1×10^4 , 1.1×10^5 , 5.5×10^4 , 3.8×10^4 and $6.8 \times 10^4 \text{ M}^{-1}$, and LODs of 2800, 3300,

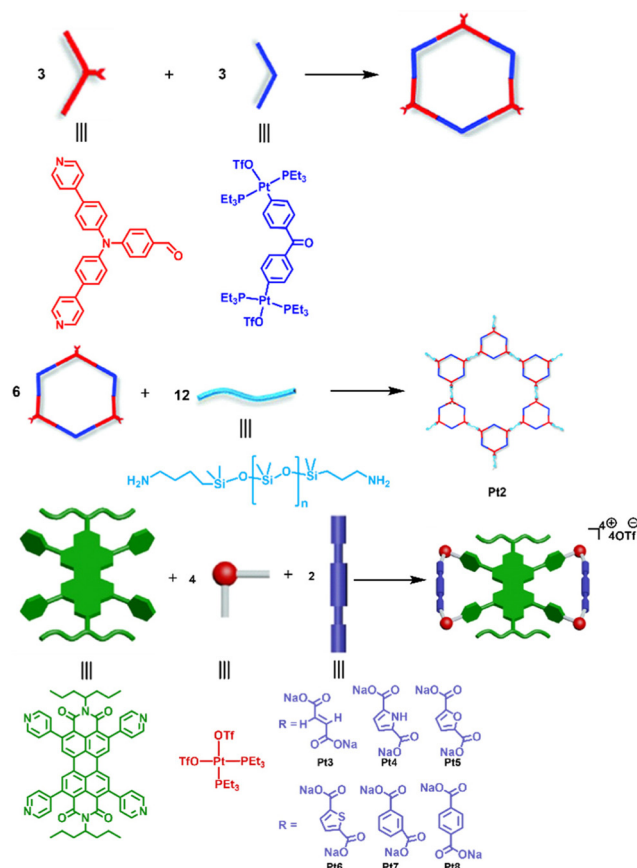


Fig. 3 Synthesis of **Pt2–Pt8**.

2500, 2400, 3000 and 2300 nM, respectively. The above results indicate that these compounds can be used as probes to detect PA.

In recent years, our group has been optimizing the detection performance of PA in aqueous media by designing Pt(II) complexes with different ligand structures. Among them, 2-phenylpyridine and its derivatives, as unique C^N-type ligands, can significantly change the luminescent properties of the corresponding complexes.^{28,29} The fluorine atom is a special element, different from other halogen elements. It has the strongest electronegativity and an atomic radius close to that of the hydrogen atom. Therefore, it is more convenient to replace the hydrogen atom to fine-tune and modify the structures of the ligands, and then effectively regulate the properties of the compounds.^{30,31}

In 2023, Yan *et al.*³² synthesized three cationic Pt(II) complexes **Pt9–Pt11**, using 2-phenylpyridine derivatives as the cyclometalating ligands and 1,10-*o*-phenanthroline as the auxiliary ligand (Fig. 4). The absolute quantum yields of **Pt10** and **Pt11** were significantly increased compared with that of the unmodified **Pt9**. **Pt9–Pt11** exhibited significant AIPE activity in H₂O/CH₃CN. **Pt9–Pt11** could be used as sensors for the effective detection of PA in aqueous media with K_{SV} values of 2.7×10^4 , 1.9×10^4 and 4.3×10^4 M⁻¹ and LODs of 170, 200 and 90 nM, respectively. These complexes exhibited excellent

selectivity in the detection of PA in complex environments. The luminescence quenching of the complexes is caused by PET.

In 2024, Yan *et al.*³³ synthesized a novel Pt(II) complex **Pt13** with 1,10-*o*-phenanthroline as the auxiliary ligand and 2-(2,4-difluorophenyl)pyridine as the cyclometalating ligand, which showed significant AIPE activity in H₂O/CH₃CN than the non-fluorinated complex **Pt12**. **Pt13** was effective in the detection of PA in H₂O/CH₃CN with respect to K_{SV} value of 2.3×10^4 M⁻¹ and LOD of 260 nM. In addition, **Pt13** showed high selectivity for the detection of PA in various water samples. Proton nuclear magnetic resonance (NMR) spectra and density functional theory (DFT) calculations indicated that the detection mechanism was attributed to PET (Fig. 4).

Introducing a trifluoromethyl group into the structures of the cyclometalating ligands can improve the solubility, thermal and oxidative stability of the corresponding complexes in organic solvents and obtain better optical properties.³⁴ In addition, the trifluoromethyl group has a unique spatial site resistance, and the fluorine atoms of the trifluoromethyl group may also form hydrogen bonds, which can affect the photophysical properties of the complexes.³⁵ In 2023, Jia *et al.*³⁶ synthesized three neutral Pt(II) complexes, **Pt14–Pt16** (Fig. 4). **Pt15** and **Pt16** with a trifluoromethyl group showed significantly higher AIPE activity in H₂O/THF than **Pt14**, suggesting that the trifluoromethyl group played a crucial role in regulating the AIPE activity. **Pt14–Pt16** have been successfully used as sensors for the detection of PA in aqueous media with K_{SV} values of 1.1×10^4 , 1.9×10^4 and 1.5×10^4 M⁻¹, and LODs of 170, 30 and 150 nM, respectively. In addition, **Pt14–Pt16** have the potential to detect PA in a variety of water samples. It has been shown that the luminescence quenching of the complexes is due to PET.

As a strong electron-donating group, the introduction of a diphenylamino (DPA) group into the metal complex could efficiently improve the photophysical properties, which has been proved to be an effective method to modulate the luminescent properties of the complexes.³⁷ In 2024, Zhang *et al.*³⁸ synthesized three neutral Pt(II) complexes **Pt17–Pt19**, with acetylacetonate as the auxiliary ligand and DPA-modified 2-phenylpyridine derivatives as the cyclometalating ligands, which exhibited AIPE properties in H₂O/THF (Fig. 4). The AIPE-active **Pt17–Pt19** have been successfully used for the detection of PA in aqueous media with K_{SV} values of 2.3×10^4 , 2.8×10^4 and 3.0×10^4 M⁻¹, and LODs of 70, 100 and 90 nM, respectively. These complexes have an excellent ability to detect PA in sophisticated environments and have potential applications in various water samples. The phosphorescence decay traces of **Pt19** were measured after adding different concentrations of PA. The results indicate that the lifetime of **Pt19** decreases continuously with increasing PA concentration. This successfully demonstrates the presence of dynamic quenching in the luminescence quenching process of **Pt19**. In addition, DFT results indicate that the sensing mechanism for the detection of PA by the three complexes can be attributed to PET.

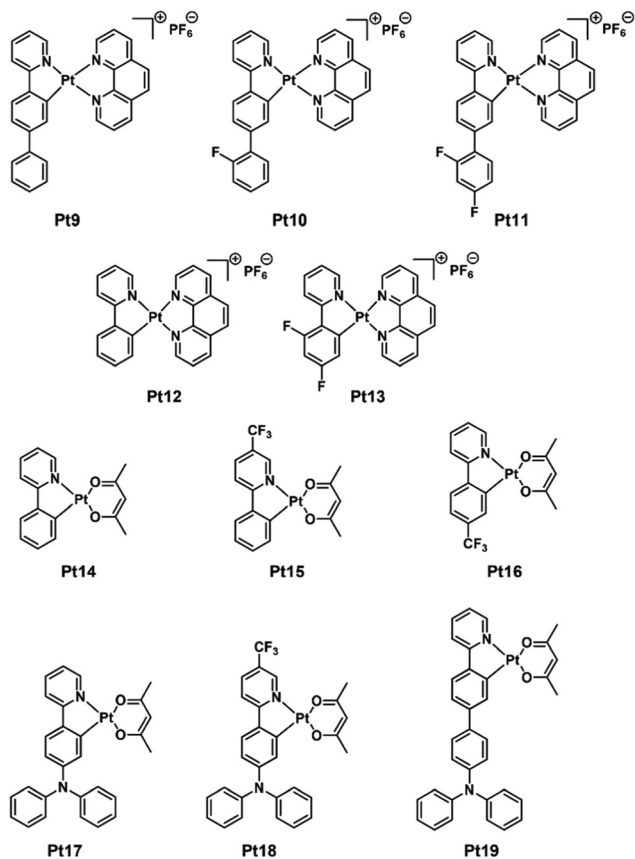


Fig. 4 Structures of **Pt9–Pt19**.

Recent advances in the detection of PA by Ir(III) complexes

Ir(III) complexes are characterized by a six-coordinated octahedral configuration, long luminescence lifetimes, large Stokes shifts, good photostability and practical synthesis routes. Like Pt(II) complexes, the luminescence performances of Ir(III) complexes can also be tuned by adjusting the ligand structures. Therefore, the development of structurally different Ir(III) complexes for PA detection has attracted great attention.^{39–41}

The carbazolyl group is a class of electron-rich groups with a large conjugation plane, and its introduction into the cyclometalating ligands can enhance the electron density of the ligands. In addition, the large conjugation planes of carbazole can easily trigger π - π interactions during molecular aggregation, which makes intermolecular bonding stronger and thus affects the luminescence performances of the complexes.^{42,43}

Regarding the study of carbazolyl-modified Ir(III) complexes for the detection of PA in organic media, in 2019, Ma *et al.*⁴⁴ synthesized a carbazole-containing yellow phosphorescent Ir(III) complex **Ir2** for the detection of nitroaromatic explosives in CH_2Cl_2 , including PA, 2,4-dinitrophenol (DNP), and 2,4-dinitrotoluene (DNT), *etc.* After adding PA, **Ir2** exhibited luminescence quenching with a K_{SV} value of $2.4 \times 10^3 \text{ M}^{-1}$ and an LOD of 29 000 nM. Since there was no spectral overlap between the UV-vis absorption of PA and the PL of **Ir2** (which is the essential prerequisite for Förster energy transfer), the quenching mechanism was assumed to be PET. In addition, paper tape testing of **Ir2**, which exhibited a significant quenching effect at low concentrations of PA, showed good potential as a solid nitroaromatic sensor (Fig. 5).

In 2020, Dong *et al.*⁴⁵ successfully synthesized a novel carbazole-containing blue luminescent Ir(III) complex **Ir3** and applied it to the detection of nitroaromatic explosives in CH_2Cl_2 . **Ir3** exhibited the highest quenching constant for the detection of PA, with a K_{SV} value of $1.9 \times 10^4 \text{ M}^{-1}$ and an LOD of 10 000 nM, demonstrating selective detection of PA. The sensing mechanism was attributed to the excited-state electron transfer based on the results of UV-vis absorption and emission spectra, as well as cyclic voltammetry (Fig. 5).

In 2024, two neutral Ir(III) complexes **Ir4** and **Ir5** modified with the electron-rich carbazole group were synthesized by Xu *et al.*⁴⁶ **Ir4** and **Ir5** exhibited AIPE properties in $\text{H}_2\text{O}/\text{THF}$ (Fig. 5). **Ir5** with a methyl group at the 5-position of the pyridine moiety of the cyclometalating ligand had stronger AIPE properties and was sensitive to the detection of PA, with a K_{SV} value of $3.7 \times 10^4 \text{ M}^{-1}$ and an LOD of 150 nM in $\text{H}_2\text{O}/\text{THF}$. The lifetime decay curves of **Ir5** after adding PA at different concentrations were recorded, and the lifetimes of **Ir5** in the presence of PA at various concentrations were fitted. The results indicate that the quenching process of **Ir5** is dynamic quenching at both low and high concentrations of PA. DFT calculations and spectroscopic results confirm that the sensing mechanism is PET.

The fluorene-based molecules have the advantages of a large conjugated system, high fluorescence quantum yield,

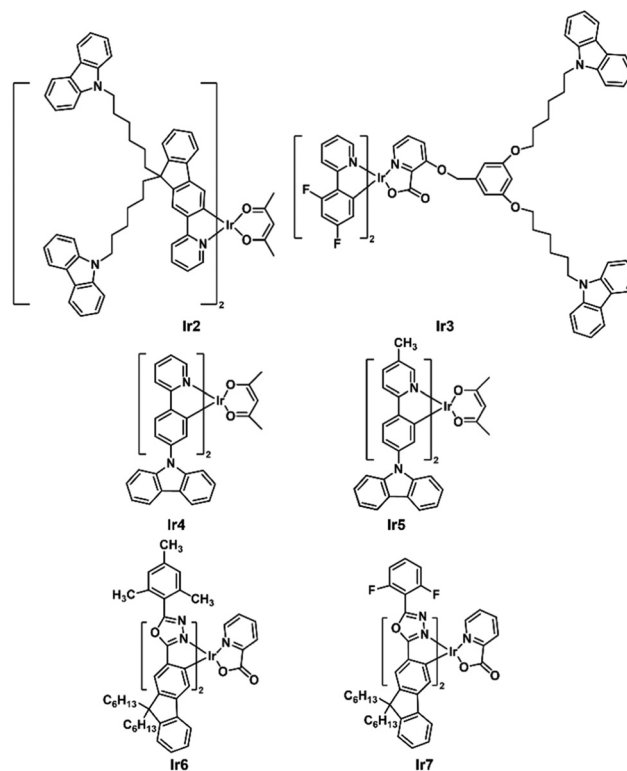


Fig. 5 Structures of **Ir2**–**Ir7**.

excellent photostability and luminescence efficiency.⁴⁷ In 2019, Liu *et al.*⁴⁸ synthesized two novel phosphorescent Ir(III) complexes **Ir6** and **Ir7** containing fluorene oxadiazole groups (Fig. 5). **Ir6** was able to detect PA with high selectivity and sensitivity in $\text{H}_2\text{O}/(\text{CH}_3)_2\text{CO}$, with a K_{SV} value of $3.4 \times 10^4 \text{ M}^{-1}$ and an LOD of 317 nM. The luminescence quenching of the complex was shown to be caused by the PET.

In recent years, our group has been working on the structure–property relationship of Ir(III) complexes and has developed a series of Ir(III) complexes with different ligand structures for the detection of PA in aqueous media. The ligand structure is dominated by 2-phenylpyridine and 2-phenylbenzothiazole and their derivatives. Among them, 2-phenylbenzothiazole is one of the commonly used ligand skeletons for the construction of Ir(III) complexes⁴⁹ due to its excellent photoluminescent properties. In 2023, He *et al.*⁵⁰ synthesized a cationic Ir(III) complex **Ir9** with a DPA-substituted 2-phenylbenzothiazole derivative as the cyclometalating ligand, which showed significant AIPE properties in $\text{H}_2\text{O}/\text{CH}_3\text{CN}$ compared to the unsubstituted **Ir8**. Both **Ir8** and **Ir9** could be used as sensors for the detection of PA in aqueous media with K_{SV} values of 7.4×10^4 and $2.6 \times 10^6 \text{ M}^{-1}$, and LODs of 50.2 and 2.2 nM, respectively. **Ir9** showed effective detection of PA, providing a higher K_{SV} value and a lower LOD. High-resolution mass spectrometry analysis and DFT calculations suggest that the sensing mechanism may be attributed to PET (Fig. 6).

As a typical electron-donating group, TPA-modified luminescent materials demonstrate strong interactions with

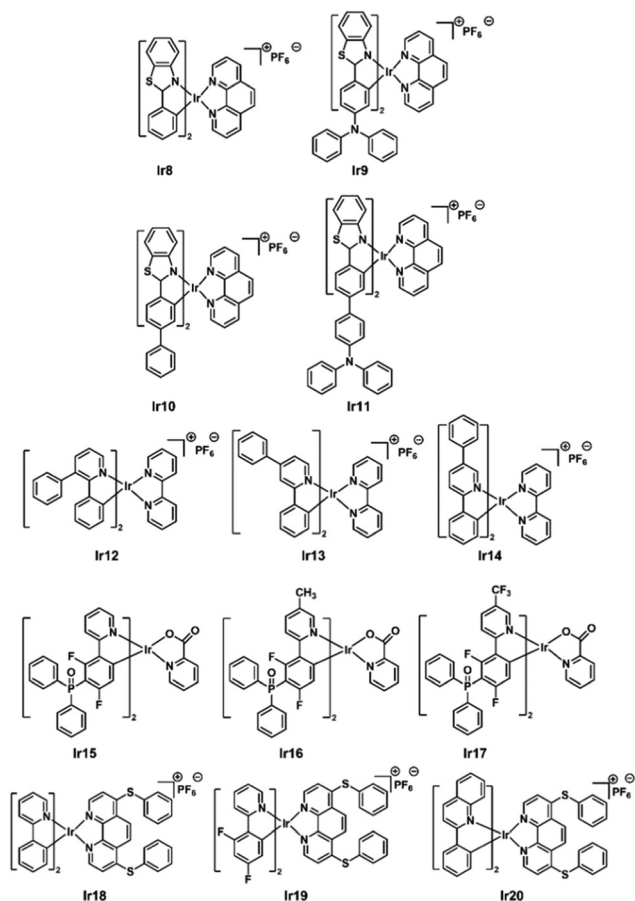


Fig. 6 Structures of Ir8–Ir20.

nitroaromatic compounds containing electron-withdrawing nitro groups.⁵¹ In 2023, He *et al.*⁵² reported two new Ir(III) complexes **Ir10–Ir11** with a phenyl or TPA group at the 4-position of the phenyl group of 2-phenylbenzothiazole, and systematically compared their emission properties with the unsubstituted complex **Ir8** (Fig. 6). These three complexes exhibited aggregation induced emission (AIE) properties⁵³ in H₂O/CH₃CN. The TPA-substituted **Ir11** showed the highest AIE activity. **Ir8**, **Ir10** and **Ir11** could be used as sensors for the detection of PA in H₂O/CH₃CN, with K_{SV} values of $7.4 \times 10^4 \text{ M}^{-1}$, $4.6 \times 10^5 \text{ M}^{-1}$ and $1.9 \times 10^6 \text{ M}^{-1}$, and LODs of 50.2, 4.6 and 2.5 nM, respectively. **Ir11** demonstrated the most effective sensing properties for the detection of PA. Proton NMR spectroscopy, high-resolution mass spectrometry analysis, and DFT calculations confirmed that the quenching mechanism of **Ir11** was induced by PET. Furthermore, the effective detection of PA in common water samples showed that **Ir8**, **Ir10** and **Ir11** could be used as promising chemical sensors.

The phenyl group, as a freely rotatable π -plane moiety, and the introduction of this group into the ligand improve the photo-physical properties of the corresponding complexes. In 2025, Yang *et al.*⁵⁴ synthesized three cationic Ir(III) complexes **Ir12–Ir14** by introducing the phenyl group at different positions of the pyridine moiety of the cyclometalating ligand (Fig. 6). All three com-

plexes exhibited typical AIPE properties in H₂O/CH₃CN. The AIPE properties were further utilized to achieve highly sensitive detection of PA in aqueous media with K_{SV} values of 2.9×10^4 , 2.3×10^4 and $1.9 \times 10^4 \text{ M}^{-1}$, and LODs of 164, 176 and 331 nM, respectively. This suggests that the phenyl group at different positions of the ligands affects the effectiveness of the corresponding complexes in PA detection. With increasing PA concentrations, the lifetimes of **Ir12–Ir14** gradually decreased, indicating the presence of dynamic quenching during the quenching process. After adding PA at different concentrations, the absorption peaks in the UV-vis absorption spectra of **Ir12–Ir14** shifted slightly, suggesting that static quenching also occurred during the quenching process. In addition, the results of proton NMR spectroscopy and spectroscopic studies suggest that the detection mechanism is mainly assigned to PET.

The diphenylphosphoryl (DPP) group is a powerful electron-withdrawing group, and the introduction of a DPP group at the corresponding position of the ligand reduces the HOMO energy of the metal complex, which enhances FRET with PA. In addition, the oxygen atom in the DPP group contributes to the specific recognition of metal ions.⁵⁵ Therefore, in 2025, Zhang and Xu *et al.*⁵⁶ reported three neutral Ir(III) complexes **Ir15–Ir17**, using DPP-substituted 2-phenylpyridine derivatives as the cyclometalating ligands (Fig. 6), which exhibited remarkable AIPE properties in H₂O/THF and were successfully used as dual-responsive luminescent sensors for the detection of PA and Fe³⁺ in aqueous media. **Ir15–Ir17** showed high efficiency and selectivity in detecting PA with K_{SV} values of 3.1×10^4 , 3.0×10^4 and $2.0 \times 10^4 \text{ M}^{-1}$, and LODs of 59, 84 and 95 nM, respectively. All complexes demonstrated excellent potential for practical applications in complicated environments. After adding PA at different concentrations, the lifetime decay traces and UV-vis absorption spectra of **Ir15** were recorded. The results indicate that there is only dynamic quenching in the luminescence quenching process of **Ir15**. The detection mechanisms for PA are attributed to PET and FRET.

In 2024, Khatua *et al.*⁵⁷ synthesized three Ir(III) complexes **Ir18–Ir20** using thiophenol-substituted 1,10-phenanthroline as the auxiliary ligands, 2-phenylpyridine, 2-(2,4-difluorophenyl)pyridine, and 2-phenylquinoline as the cyclometalating ligands, respectively (Fig. 6). **Ir18–Ir20** were used for the selective detection of PA in H₂O/CH₃CN with LODs of 0.6, 0.3, and 3.8 nM and K_{SV} values of 8.4×10^5 , 5.7×10^6 and $4.5 \times 10^5 \text{ M}^{-1}$, respectively. PL studies show that the luminescence quenching of these complexes is highly selective towards PA over other nitroaromatic compounds and metal ion-based quenching agents. After adding PA, the average excited-state lifetimes of **Ir18–Ir20** all decreased, indicating the presence of dynamic quenching. Finally, with the help of spectroscopic analyses and DFT calculations, the quenching mechanism is attributed to PET.

Conclusion and outlook

In summary, we systematically review the recent advances in Pt(II) and Ir(III) complexes for PA detection and summarize the

performance differences (sensitivity, selectivity, quenching efficiency) of metal complexes with different ligand designs (introducing groups such as DPA, TPA and $-CF_3$) in detecting PA (Tables 1 and 2). The photophysical properties and the sensing performances of the complexes could be easily modified by modulating the structures of the ligands. Among them, the complexes containing a DPA group or a TPA group exhibited excellent detection performances in aqueous media, with LODs down to the nM level and K_{SV} values up to $10^6 M^{-1}$. It was shown that these complexes mainly achieved the efficient detection of PA through PET and/or FRET mechanisms.

Although the metal complexes have made significant progress in the detection of PA, the existing systems still face the following challenges. (1) Many metal complexes exhibit low chemical stability, solubility, and luminescence performance in aqueous or complicated environmental media. These complexes easily undergo aggregation, precipitation, or ligand dissociation, leading to unstable signals. In common environmental samples (e.g., soil leachates, industrial wastewater), interfering factors such as coexisting ions, organic matter, and pH variations further affect detection accuracy and reliability. (2) Many reported metal complex sensors exhibit responses to multiple nitroaromatic compounds, yet their specific recognition capability for PA remains limited. (3) There is a reliance on laboratory equipment for practical applications, with portability and anti-interference capabilities that need to be further improved. (4) There is a need to transcend superficial studies of structure–property correlations, conducting in-depth exploration to elucidate how specific structural features influence sensing performance.

Aiming at the current technical bottlenecks of Pt(II) or Ir(III) complexes in the detection of PA, future research can make breakthroughs from the following multi-dimensional aspects: firstly, the development of novel stabilized ligand systems through molecular engineering strategies, which can enhance the chemical stability of the complexes in complicated aqueous environments. Secondly, the design of molecular structures is guided by DFT calculations, and the structures with specific recognition for PA are constructed by precisely regulating the electronic effects and spatial site resistance of the ligand substituents. Thirdly, the AIPE-active metal complexes at the aggregated state play a crucial role in the detection of PA in aqueous media. By controlling the self-assembly process, luminescent aggregates with specific nanostructures are expected to demonstrate high performance in the detection of PA. Furthermore, the combination of high-performance complexes and portable devices can achieve rapid on-site detection, and even direct “naked-eye” results through color changes. It is noteworthy that exploring the synergistic sensing mechanism based on the MOF system, realizing the detection of explosives with high sensitivity and high selectivity, and combining the dynamic fluorescence response characteristics of the composite system can open up new paths for the construction of a new type of multifunctional sensing system.⁵⁸ These innovative directions will promote the development of explosives detection technology in the direction of high sensi-

tivity, high selectivity and intelligence, which will show important application value in the fields of environmental monitoring and anti-terrorism security.

Author contributions

Xiaoran Yang: literature search, investigation, and writing – original draft; Qinglong Zhang and Boyuan Miao: literature search, formal analysis, and writing; and Chun Liu: conceptualisation, supervision, writing – review & editing, and correspondence. All authors have read and approved the final manuscript.

Conflicts of interest

There are no conflicts to declare.

Data availability

No new data are presented in the manuscript; all data are taken from the primary literature.

Acknowledgements

The authors thank the financial support from the National Natural Science Foundation of China (21978042) and the Fundamental Research Funds for the Central Universities (DUT22LAB610).

References

- 1 P. Ghorai, A. Hazra, J. Mandal, S. Malik, P. Brandão, P. Banerjee and A. Saha, *Inorg. Chem.*, 2023, **62**, 98–113.
- 2 H. Wang, C. Chen, Y. Liu, Y. Wu, Y. Yuan and Q. Zhou, *Talanta*, 2019, **198**, 242–248.
- 3 P. Singh, A. Mukherjee, A. Mahato, A. Pramanik and D. Dhak, *Chem. Afr.*, 2023, **6**, 561–578.
- 4 F. Ghasemi and M. R. Hormozi-Nezhad, *Talanta*, 2019, **201**, 230–236.
- 5 C. Zhu, H. Huang and Y. Chen, *Environ. Pollut.*, 2022, **307**, 119570.
- 6 P. Li, X. Li and W. Chen, *Curr. Opin. Electrochem.*, 2019, **17**, 16–22.
- 7 J. Estevanes and G. Monjardez, *Forensic Sci. Int.*, 2024, **365**, 112292.
- 8 Y. Zhang, X. Ma, S. Zhang, C. Yang, Z. Ouyang and X. Zhang, *Analyst*, 2009, **134**, 176–181.
- 9 D. Noh and E. Oh, *Polymers*, 2024, **16**, 908.
- 10 X. Liu, Y. Han, Y. Shu, J. Wang and H. Qiu, *J. Hazard. Mater.*, 2022, **425**, 127987.

- 11 V. Sathish, A. Ramdass, M. Velayudham, K.-L. Lu, P. Thanasekaran and S. Rajagopal, *Dalton Trans.*, 2017, **46**, 16738–16769.
- 12 Z. Zuo, X. Pan, G. Yang, Y. Zhang, X. Liu, J. Zha and X. Yuan, *Dalton Trans.*, 2023, **52**, 2942–2947.
- 13 B. Li, Z. Liang, H. Yan and Y. Li, *Mol. Syst. Des. Eng.*, 2020, **5**, 1578–1605.
- 14 S. K. Patra, B. Sen, M. Rabha and S. Khatua, *New J. Chem.*, 2022, **46**, 169–177.
- 15 S. Ghosh and P. S. Mukherjee, *Organometallics*, 2008, **27**, 316–319.
- 16 G.-G. Shan, H.-B. Li, H.-Z. Sun, D.-X. Zhu, H.-T. Cao and Z.-M. Su, *J. Mater. Chem. C*, 2013, **1**, 1440–1449.
- 17 C. Chen, Y. Xu, Y. Wan, W. Fan and Z. Si, *Eur. J. Inorg. Chem.*, 2016, **2016**, 1340–1347.
- 18 F. Zu, F. Yan, Z. Bai, J. Xu, Y. Wang, Y. Huang and X. Zhou, *Microchim. Acta*, 2017, **184**, 1899–1914.
- 19 X. Liu, P. Lei, X. Liu, Y. Li, Y. Wang, L. Wang, Q.-D. Zeng and Y. Liu, *Polym. Chem.*, 2023, **14**, 2979–2986.
- 20 D. Escudero, *Acc. Chem. Res.*, 2016, **49**, 1816–1824.
- 21 S. Nishiyama, J. Ochi and K. Tanaka, *Asian J. Org. Chem.*, 2025, **14**, e202400513.
- 22 H. Zong, X. Wang, X. Mu, J. Wang and M. Sun, *Chem. Rec.*, 2019, **19**, 818–842.
- 23 M. K. Mahto, D. Samanta, M. Shaw, M. A. S. Shaik, R. Basu, I. Mondal, A. Bhattacharya and A. Pathak, *ACS Appl. Nano Mater.*, 2023, **6**, 8059–8070.
- 24 Q. Wan, X.-S. Xiao, W.-P. To, W. Lu, Y. Chen, K.-H. Low and C.-M. Che, *Angew. Chem., Int. Ed.*, 2018, **57**, 17189–17193.
- 25 C. Liu, X. Song, X. Rao, Y. Xing, Z. Wang, J. Zhao and J. Qiu, *Dyes Pigm.*, 2014, **101**, 85–92.
- 26 Y. Hou, S. Li, Z. Zhang, L. Chen and M. Zhang, *Polym. Chem.*, 2020, **11**, 254–258.
- 27 Y. Hou, R. Shi, H. Yuan and M. Zhang, *Chin. Chem. Lett.*, 2023, **34**, 107688.
- 28 L. Niu, G. Ren, T. Hou, X. Shen and D. Zhu, *Inorg. Chem. Commun.*, 2021, **130**, 108737.
- 29 H. R. Shahsavari and S. Paziresh, *New J. Chem.*, 2021, **45**, 22732–22740.
- 30 L. Wang, Z. Gao, C. Liu, Y. Chen, W. Tao and L. Lu, *Tetrahedron*, 2020, **76**, 131390.
- 31 S. Dehnen, L. L. Schafer, T. Lectka and A. Togni, *Inorg. Chem.*, 2021, **60**, 17419–17425.
- 32 Y. Yan, W. Jia, L. Zhang and C. Liu, *Dyes Pigm.*, 2023, **220**, 111719.
- 33 Y. Yan, W. Jia, R. Cai and C. Liu, *Chin. Chem. Lett.*, 2024, **35**, 108819.
- 34 M. G. Dhara and S. Banerjee, *Prog. Polym. Sci.*, 2010, **35**, 1022–1077.
- 35 W. Tao, Y. Chen, L. Lu and C. Liu, *Tetrahedron Lett.*, 2021, **66**, 152802.
- 36 W. Jia, Y. Yan, R. Cai, Q. Yin, P. He and C. Liu, *Tetrahedron Lett.*, 2023, **126**, 154663.
- 37 D. Wang, T.-F. Shao, S.-M. Li, W. Cao, Q. Yao and Y. Ma, *Dyes Pigm.*, 2024, **226**, 112114.
- 38 Q. Zhang, Y. Yan, R. Cai, X.-N. Li and C. Liu, *Materials*, 2024, **17**, 4366.
- 39 S. Aoki, K. Yokoi, Y. Hisamatsu, C. Balachandran, Y. Tamura and T. Tanaka, *Top. Curr. Chem.*, 2022, **380**, 36.
- 40 M. R. Schreier, X. Guo, B. Pfund, Y. Okamoto, T. R. Ward, C. Kerzig and O. S. Wenger, *Acc. Chem. Res.*, 2022, **55**, 1290–1300.
- 41 Q. Zhang, Y. Chen and C. Liu, *Mol. Chem. Eng.*, 2025, **1**, 100008.
- 42 K. Brunner, A. van Dijken, H. Börner, J. J. A. M. Bastiaansen, N. M. M. Kiggen and B. M. W. Langeveld, *J. Am. Chem. Soc.*, 2004, **126**, 6035–6042.
- 43 H.-T. Mao, Y. Yang, K.-Y. Zhao, Y.-C. Duan, W.-L. Song, G.-G. Shan and Z.-M. Su, *Dyes Pigm.*, 2021, **192**, 109439.
- 44 Q. Ma, W. Dong, Z. Ma, X. Lv, Y. Li and Q. Duan, *Mater. Lett.*, 2019, **249**, 120–123.
- 45 W. Dong, Q. Ma, Z. Ma, Q. Duan, X. Lü, N. Qiu, T. Fei and Z. Su, *Dyes Pigm.*, 2020, **172**, 107799.
- 46 J. Xu, L. Zhang, Y. Shi and C. Liu, *Sensors*, 2024, **24**, 4074.
- 47 Y. Qu and Y. Li, *J. Mol. Struct.*, 2025, **1330**, 141466.
- 48 J.-W. Liu, Y.-N. Xu, C.-Y. Qin, Z.-N. Wang, C.-J. Wu, Y.-H. Li, S. Wang, K. Y. Zhang and W. Huang, *Dalton Trans.*, 2019, **48**, 13305–13314.
- 49 D. Liu, H. Ren, L. Deng and T. Zhang, *ACS Appl. Mater. Interfaces*, 2013, **5**, 4937–4944.
- 50 P. He, Y. Chen, X.-N. Li, Y.-Y. Yan and C. Liu, *Dalton Trans.*, 2023, **52**, 128–135.
- 51 E. V. Verbitskiy, Y. A. Kvashnin, A. A. Baranova, K. O. Khokhlov, R. D. Chuvashov, I. y. E. Schapov, Y. A. Yakovleva, E. F. Zhilina, A. V. Shchepochkin, N. I. Makarova, E. V. Vetrova, A. V. Metelitsa, G. L. Rusinov, O. N. Chupakhin and V. N. Charushin, *Dyes Pigm.*, 2020, **178**, 108344.
- 52 P. He, Y. Chen, X.-N. Li, Y.-Y. Yan and C. Liu, *Chemosensors*, 2023, **11**, 177.
- 53 G. Zhang, X. Fu, D. Zhou, R. Hu, A. Qin and B. Z. Tang, *Smart Mol.*, 2023, **1**, e20220008.
- 54 X. Yang, J. Du, R. Cai and C. Liu, *Sensors*, 2025, **25**, 839.
- 55 T. Verma, P. Verma and U. P. Singh, *Microchem. J.*, 2023, **191**, 108771.
- 56 Q. L. Zhang, J. C. Xu, Q. Xu and C. Liu, *Chemosensors*, 2025, **13**, 1.
- 57 M. Rabha, D. L. Lyngkhai, S. K. Patra and S. Khatua, *Inorg. Chem. Front.*, 2024, **11**, 1434–1449.
- 58 Y. Jia, X. Wang, H. Li and C. He, *Chemosensors*, 2025, **13**, 3.